International Journal of Thermal Sciences 78 (2014) 1–8

Contents lists available at ScienceDirect

International Journal of Thermal Sciences

journal homepage: www.elsevier.com/locate/ijts

Heat transfer of a circular impinging jet on a circular cylinder in crossflow

X.L. Wang [a], D. Motala [b], T.J. Lu [a], S.J. Song [c], T. Kim [b,*]

[a] State Key Laboratory for Mechanical Structure Strength and Vibration, Xi'an Jiaotong University, Xi'an 710049, China
[b] School of Mechanical Engineering, University of the Witwatersrand, Johannesburg Wits 2050, South Africa
[c] School of Mechanical and Aerospace Engineering, Seoul National University, Seoul 151-742, South Korea

ARTICLE INFO

Article history:
Received 14 April 2013
Received in revised form
5 November 2013
Accepted 5 November 2013
Available online 18 December 2013

Keywords:
Circular cylinder
Circumferential heat transfer
Impinging circular jet
Flow separation
Transition

ABSTRACT

Local heat transfer characteristics on a circular cylinder subject to a circular impinging jet in crossflow are studied experimentally at a fixed jet Reynolds number of $Re_j = 20{,}000$. Three cylinder-to-jet diameter ratios, $D/D_j = 0.5$, 2.0, and 5.0 are selected for a fixed jet diameter D_j. As reference, heat removal from a flat plate (having $D/D_j = \infty$) by the same circular impinging jet is also measured. Results reveal that local surface heat transfer characteristics are governed separately by the mechanisms for two limiting configurations. Smaller cylinders (than the circular jet diameter e.g., $D/D_j \leq 0.5$) behave as if immersed in uniform free-stream – flow separation causes the local minimum heat transfer. Larger cylinders (than the circular jet diameter e.g., $D/D_j \geq 2.0$) follow the local heat transfer characteristics observable on a flat plate subject to a circular impinging jet – laminar to turbulent flow transition induces local heat transfer peaks.

1. Introduction

Impinging jet cooling (or heating) has long been studied due to its superior heat transfer capability to other convective heat transfer schemes. A circular impinging jet on a flat plate serves as a fundamental configuration amongst others. Consequently, a multitude of studies have been devoted to this configuration [1–5]. Some of the conclusions drawn are summarized as: (a) the highest heat transfer on a flat plate typically occurs at the stagnation point whose magnitude varies with jet exit-to-flat plate spacing (or referred to an impinging distance) at low turbulence levels [4] and low Reynolds numbers [6] and (b) depending on the impinging distance relative to the potential core of jet flow, either two peaks of local heat transfer (a primary peak at the stagnation point and a second peak off from the stagnation point) or a single peak (only a primary peak at the stagnation point) exists.

In some engineering applications, a target surface has a finite radius (e.g., circular cylinders and convex surfaces)) such as the cooling of a circular furnace containing the melt of metal slurry with gaseous pores during the closed-cell foaming process (e.g., via the direct foaming method) [7,8] (see Fig. 1). In this particular application, many parameters are known to affect the quality of final foam products including those associated with the furnace cooling. The circular furnace experiences two distinctive upstream flow conditions (depending on its relative location to the potential core of cooling jet flow): uniform-like (inside the potential core) and shear (outside the potential core) flows. Furthermore, a diameter ratio between the cooling jets and the circular furnace may also play an important role in the local thermal flow characteristics on the furnace surface, which differentiates the present configuration from impinging circular jets on a flat plate.

Gau and Chung [9] who investigated the heat transfer characteristics of semi-cylindrical convex surfaces (with a diameter of D) subject to slot jet cooling with a slot width of b, observed that decreasing the ratio of D/b enhances heat transfer at the stagnation point, arguing that the increased counter-rotating vortex size is responsible. Cornaro et al. [10] conducted heat transfer experiments on jet impingement cooling on convex semi-cylindrical surfaces and observed that the stagnation Nusselt number increases with decreasing D/D_j. Lee et al. [11] examined local heat transfer on convex surfaces subject to a round impinging jet and reported that the stagnation Nusselt number increases with decreasing D/D_j.

Experimental results contradicting those discussed above have also been reported by Sparrow et al. [12] who used a naphthalene mass transfer technique to measure mass transfer coefficients on a

* Corresponding author. Tel.: +27 11 717 7359.
E-mail address: tongbeum@gmail.com (T. Kim).

1290-0729/$ – see front matter © 2013 Elsevier Masson SAS. All rights reserved.
http://dx.doi.org/10.1016/j.ijthermalsci.2013.11.005

Nomenclature

C_p	static pressure coefficient defined in Eq. (2)
D	target circular cylinder diameter, m
D_j	circular jet diameter, m
h	convection heat transfer coefficient, W/(m^2 K)
k_f	thermal conductivity of air, W/(m K)
Nu	Nusselt number based on a jet diameter defined in Eq. (3)
p_e	static pressure measured at a jet exit ($z = 0$), Pa
$p(\alpha)$	pressure measured at an arbitrary azimuth angle (α), Pa
Pr	Prandtl number
r	radial coordinate
Re_j	Reynolds number based on a jet diameter defined in Eq. (1)
s	a lateral distance from the stagnation point of a target cylinder along the S-axis, m; inflection point
S	coordinate along the circumference of a cylinder
T_j	jet temperature measured at a jet exit, K
T_s	local temperature measured on a circular cylinder, K
w	axial velocity component of a circular jet, m/s
w_e	jet exit velocity at $r = 0$ and $z = 0$, m/s
w_0	centerline (axial) velocity at $r = 0$, m/s
z	a distance along a jet axis from a jet exit to a stagnation point on a cylinder, m
Z	axial coordinate coinciding with a jet axis
Z'	coordinate coinciding with a target cylinder axis
α	an azimuth angle measured from the stagnation point of a cylinder, degree
ρ	density of air, kg/m^3
μ	viscosity of air, kg/(m s)

circular cylinder subject to a circular impinging jet. Both the stagnation point and circumferential distributions on a cylinder surface were measured. The stagnation mass transfer was increased with increasing D/D_j at a fixed impinging distance and jet Reynolds number. Tawfek [13] investigated circumferential and axial heat transfer distributions on an isothermal circular cylinder subject to a round impinging jet. The results showed that the increased cylinder diameter enhances the stagnation heat transfer. Singh [14] experimentally and numerically investigated a circular air impinging jet on a cylinder. It was observed that the stagnation heat transfer increases as the diameter ratio D/D_j increases, as opposed to the findings reported in Refs. [9–11], as summarized in Table 1.

Thus far, observations made on circumferential heat transfer characteristics on a circular cylinder (or a convex surface) impinged by a circular single jet are: (a) when positioned close to the jet exit, a second peak, in addition to a primary peak at the stagnation point, forms and (b) a second peak disappears when positioned relatively far away from the jet exit along the jet axis [9–13]. Despite numerous efforts including those discussed above, some thermophysics has not been fully understood regarding local heat transfer at the stagnation point and along the circumference of a circular cylinder (or convex surface) subject to a circular impinging jet. Specific issues to be squarely addressed are:

(a) how a target cylinder-to-jet diameter ratio affects the dependence of the stagnation heat transfer on an impinging distance, and
(b) how the presence of the potential core of a circular jet (i.e., its relative location to the impinging distance) alters local heat transfer characteristics on a cylinder surface.

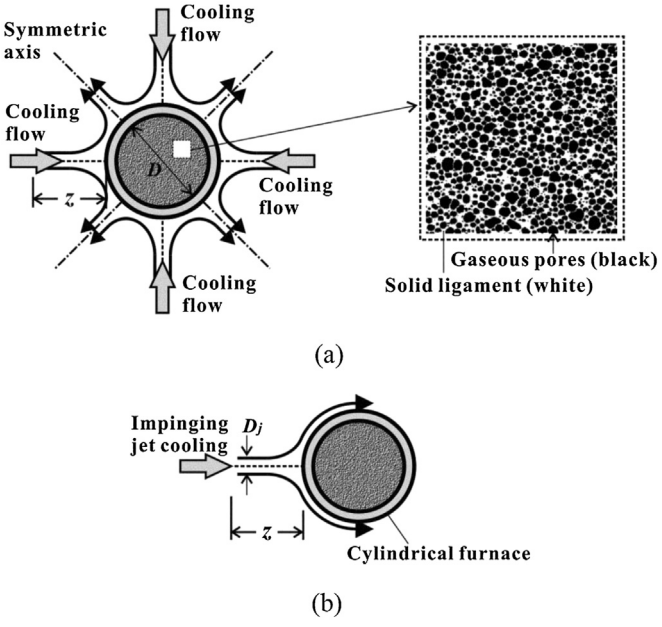

Fig. 1. Schematic of furnace cooling: (a) multiple impinging jet cooling of a cylindrical furnace containing metal melt with closed-cell pores; (b) single impinging jet cooling as a simplified configuration of (a).

2. Experimental details

2.1. Test rig and instrumentation

A series of experiments on a circular cylinder of diameter D positioned at two distinctive locations (inside and outside the potential core of jet flow) have been conducted for a fixed jet Reynolds number of $Re_j = 20{,}000$. As reference, the circular jet removing heat from a flat plate (i.e., $D = \infty$) is also considered. Three selected cylinder diameters $D/D_j = 0.5$, 2.0, and 5.0 are tested for a fixed D_j in addition to the flat plate (Fig. 2). Detailed dimensions are listed in Table 2. Static pressure and heat transfer coefficients along the circumference of each cylinder are measured. Prior to pressure and heat transfer measurements, the potential core length of the present circular jet flow is measured.

Fig. 3 shows a schematic of the present test facility. Air at ambient conditions drawn by a centrifugal fan is discharged from a circular jet nozzle with a fixed inner diameter of $D_j = 30$ mm. The mass flow rate measured by an orifice plate is adjusted to fix the jet Reynolds number Re_j (Eq. (1)) at 20,000. An acrylic (target) circular cylinder ($k_s \sim 0.02$ W/mK) is mounted on a linear traverse system to vary the impinging distance systematically.

To quantify the potential core length, the centerline velocity of the jet flow is measured using a Pitot tube which is mounted on an automated linear traverse system along the Z-axis. Pressure readings from the stagnation and static tappings are recorded by a differential pressure transducer (DSA™, Scanivalve Inc.). To obtain the circumferential variation of static pressure on the cylinder surface, a static pressure tapping (inner diameter of 0.5 mm) is drilled into the cylinder surface and the cylinder is rotated in a 2.5° increment to cover the circumferential range from $\alpha = 0°$ (stagnation point) to $\alpha = 180°$.

Table 1
Summary of conclusions drawn on dependence of stagnation heat transfer upon relative curvature of a heated circular cylinder/sphere subjected to impingement jet cooling where D is the cylinder diameter, D_j is the circular jet diameter and the Z-axis coincides with the jet axis.

Reference	Jet Reynolds number, Re_j	Potential core length, L_p	z/D_j	D/D_j	Conclusion: Stagnation heat transfer increases with:
Gau and Chung [9]	6000–350,000 (Slot jet with width b)	Less than $4.0b$ (inferred from flow images)	2.0–16.0	8.0–45.7	Decreasing D/b
Cornaro et al. [10]	6000–16,000 (Round jet)	$4.0D_j$–$5.6D_j$	1.0–4.0	2.6–5.5	Decreasing D/D_j
Lee et al. [11]	11,000–50,000 (round jet)	$3.1D_j$–$4.2D_j$	2.0–10.0	11–29	Decreasing D/D_j
Sparrow et al. [12]	4000–25,000 (Round jet)	N/A	5.0–15.0	2.3–5.3	Increasing D/D_j
Tawfek [13]	3800–40,000 (Round jet)	N/A	7.5–30.0	7.1–16.7	Increasing D/D_j
Singh et al. [14]	10,000–25,000 (Round jet)	N/A	4.0–16.0	4.0–9.0	Increasing D/D_j

To impose constant heat flux on the cylinder surface, a film-type heating element with a thickness 0.32 mm is used. Double-sided adhesive tape is inserted between the heating element and the cylinder surface. To directly measure the heat flux removed from the heating element by the jet flow, a film heat flux gauge, 0.15 mm thick, is used. Also, to measure the local temperature along the cylinder circumference, a thin film T-type thermocouple (0.04 mm in thickness) is flush mounted on the cylinder surface at a cylinder mid-span, coinciding with the jet axis. To cover half of the cylinder circumference from $\alpha = 0^\circ$ to $\alpha = 180^\circ$, the cylinder is rotated with a 2.5° increment. Note that no flow disturbance or change by the surface mounted film thermocouples is assumed due to their thinness. At each angle, the experiment is run for half an hour to reach steady state temperature values. A bead T-type thermocouple is used to monitor the jet exit temperature (T_j). Prior to the measurements, each thermocouple is calibrated in a container filled with an ice–water mixture.

2.2. Data reduction parameters and measurement uncertainties

The jet Reynolds number, based on the jet diameter D_j and centerline jet velocity w_e measured at the jet exit is defined as:

$$Re_j = \rho w_e D_j / \mu \tag{1}$$

During the entire experiment, the jet Reynolds number is fixed at 20,000.

The local static pressure distribution is evaluated using the dimensionless pressure coefficient defined as:

$$C_p = \frac{p(\alpha) - p_e}{\rho w_e^2/2} \tag{2}$$

where $p(\alpha)$ and p_e are the static pressures measured on the cylinder surface at an arbitrary azimuth angle (α) and at the jet exit, respectively.

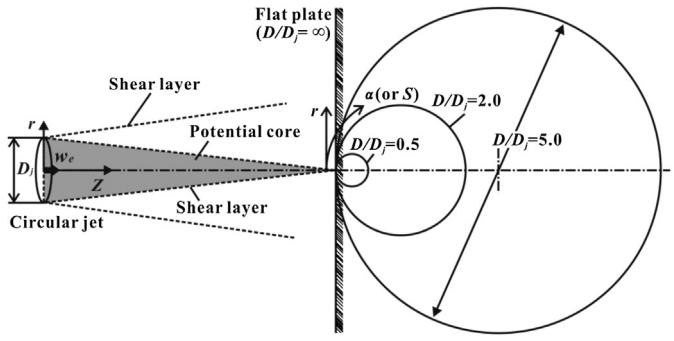

Fig. 2. Description of circular jet flow impinging on circular bodies in crossflow with different diameter ratios (D/D_j) where a flat plate has an infinite diameter ratio (i.e., $D = \infty$).

The heat transfer characteristics are evaluated using the Nusselt number with the jet diameter D_j defined as:

$$Nu(\alpha) = h(\alpha) D_j / k_f \tag{3}$$

where

$$h(\alpha) = q'' / (T_s(\alpha) - T_j) \tag{4}$$

Here, q'' is the heat flux emitted from the cylinder surface measured by a film heat flux gauge flush-mounted on the cylinder surface, k_f is the thermal conductivity of air whilst $T_s(\alpha)$ and T_j are the temperatures measured along the cylinder circumference at an arbitrary azimuth angle α and at the jet exit $z = 0$, respectively. The origin of the azimuth angle α coincides with the stagnation point.

In numerous previous studies of heat transfer around a cylinder that is immersed in a uniform free-stream, it is common to define non-dimensional parameters such as the Reynolds and Nusselt numbers as a function of the cylinder diameter, whereas a jet diameter is a conventional characteristic length for impinging jet heat transfer on a flat plate. Since results on a flat plate subject to an impinging jet are compared as reference, a length scale common for these two limiting cases, i.e., a jet diameter (D_j) appears to be a reasonable choice, thus adopted as a characteristic length scale in the present study.

The uncertainty associated with the azimuth angle is within $\pm 0.2^\circ$. The measurement uncertainty of the jet Reynolds number and the static pressure coefficient is estimated using a method reported in Ref. [15] (based on 20:1 odds) and is within 1.3% and 1.7%, respectively. The resolution of the temperature readings from the temperature scanner is ± 0.1 K for each thermocouple. For heat flux measurement, the error associated with the voltmeter is estimated to be less than ± 5 μV, resulting in an error less than ± 6 W/m^2 for heat flux (0.4%). Thus, the uncertainty of the Nusselt number is calculated to be within 4.7%.

3. Discussion of results

3.1. Circular jet characteristics in a free exit

According to the classical description of free jet flow structures [16], there exist three distinctive flow regions: (a) the initial region,

Table 2
Parameters of test setup and conditions.

Test parameter	Value
Circular jet diameter, D_j	0.03 m
Relative curvature, D/D_j	0.5, 2.0, 5.0, flat plate (∞)
Reynolds number, Re_j	20,000
Circular cylinder span, S	0.48 m
Width of heating element, S_h	0.20 m
Constant heat flux, q''	1350 W/m^2

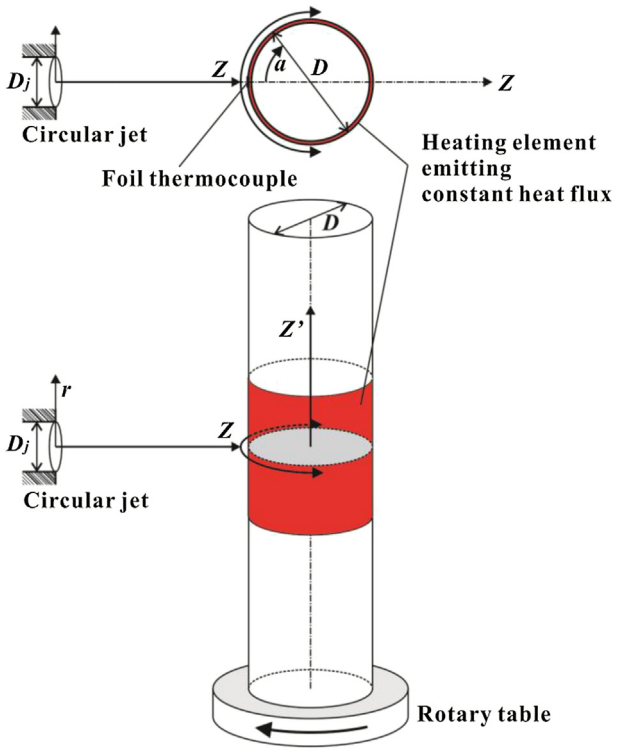

Fig. 3. Schematic of test setup for measuring heat transfer distribution along the circumference of a heated circular cylinder cooled by circular impinging jet.

(b) the transitional region, and (c) the fully developed region. In the initial region, the jet velocity along the jet axis maintains its magnitude as high as that at the jet exit. Furthermore, the jet flow is undisturbed by the flow interaction with the surrounding fluid at rest (submerged jet), whose core region is termed the "potential core." For circular jets, Martin [1] suggested that the potential core length is about $4D_j$ whilst Gautner [3] reported that the core length typically ranges from $4.7D_j$ to $7.7D_j$. After the jet flow is fully developed via transition, the axial velocity profiles become self-similar, collapsing onto a single curve that could be fitted using the Gaussian distribution [5].

The potential core length of the present circular jet in the free exit is characterized first by traversing the centerline jet velocity w_0 (i.e., at $r = 0$). Fig. 4 shows the centerline velocity normalized by that measured at the jet exit, w_e. Following the definition of Giralt et al. [17] that the potential core length is the distance from a nozzle exit to an axial point where the centerline velocity w_0 is 98% of the jet exit velocity w_e, it is derived from Fig. 4 that the present potential core persists up to $z/D_j = 4.0$. Inside the potential core ($z/D_j \leq 4.0$), the centerline velocity has the same magnitude as w_e. Outside the potential core (i.e., $z/D_j > 4.0$), the axial centerline velocity w_0 decays inversely proportional to the axial distance [16], as:

$$w_0/w_e \sim (z/D_j)^{-1} \quad (5)$$

The measured centerline velocity data follows the trend expressed by Eq. (5) after $z/D_j = 8.0$. According to Abramovich [16], the onset of the fully developed region (or self-similar region) occurs approximately at $z/D_j = 8.0$.

It should be noted that the velocity characteristics of the present jet in the free exit (Fig. 4) are expected to vary due to the presence of a target circular cylinder placed downstream, but assumed to be consistent amongst the selected cases. The jet flow structure affected by the presence of a target surface is limited within

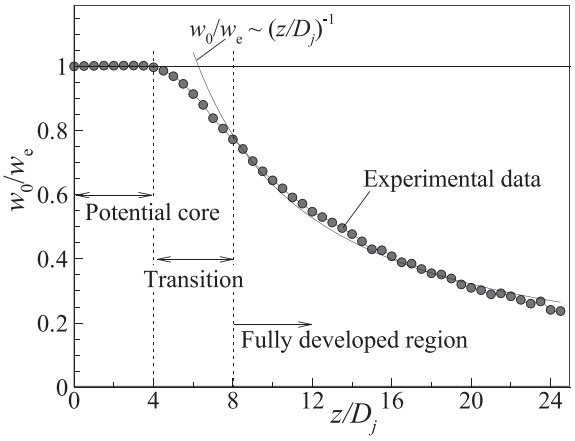

Fig. 4. Free jet characteristics at $Re_j = 20{,}000$ showing axial variation of normalized centerline velocity, w_0/w_e, indicating a potential core persisting up to $z/D_j = 4.0$.

approximately $1.0D_j$ upstream and other flow regions remain unaffected [6,18], which argument may hold for the present configuration.

3.2. Crossflow consideration

This study only considers heat transfer characteristics in a single plane as illustrated in Fig. 2 (i.e., a crossflow plane) although the flow discharged from circular jets interacting with a target cylinder

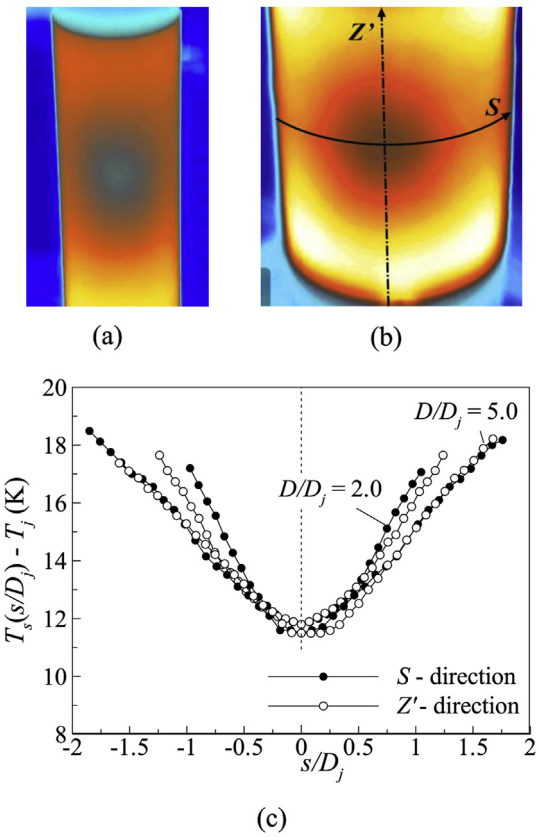

Fig. 5. Temperature distribution on a circular cylinder subject to circular impinging jet for $Re_j = 20{,}000$ at $z/D_j = 8.0$ (outside the potential core) by an infrared (IR) camera; (a) temperature contour for $D/D_j = 2.0$; (b) temperature contour for $D/D_j = 5.0$; (c) comparison of temperature distributions along the S-direction and the Z'-direction.

is three-dimensional. Unlike a circular jet impinging on a flat plate whose thermal flow field is axisymmetric, the crossflow consideration simplifies the actual three-dimensional problem.

The overall temperature contours on the two selected cylinders are shown in Fig. 5(a) for $D/D_j = 2.0$ and in Fig. 5(b) for $D/D_j = 5.0$, captured by a pre-calibrated infrared (IR) camera. The impinging distance was set to be $z/D_j = 8.0$ at $Re_j = 20{,}000$. Isothermal lines on the cylinder ($D/D_j = 2.0$) form an ellipse-like shape; slightly wider in the Z'-direction (coinciding with the target cylinder's axis) than in the S-direction (along the circumference). On a bigger cylinder ($D/D_j = 5.0$), isothermal lines turn to a circular shape.

To quantify this, the temperature data was extracted along the two selected directions and the results are plotted in Fig. 5(c). On the two cylinders i.e., $D/D_j = 2.0$ and 5.0, the temperature distribution, at least, along these two directions is almost identical whereas there is a deviation on the smaller cylinder surface ($D/D_j = 2.0$) where a slightly steeper temperature drop exists along the circumference (the S-direction) than that along the Z'-direction. The crossflow consideration simplifies the three-dimensional heat transfer analysis but may provide useful information on the present problem: circular impinging jet heat transfer on a long circular cylinder.

3.3. Convective heat transfer at the stagnation point ($\alpha = 0°$)

Heat transfer at the stagnation point of a cylinder with three selected diameter ratios, $D/D_j = 0.5$, 2.0, and 5.0 is measured whilst the impinging distance (z/D_j) is varied from 1.0 to 10.0. Results in Fig. 6 show that as the cylinder is moved away from the jet exit along the jet axis (the Z-axis), the stagnation heat transfer is increased whilst peaking at $6.0 \le z/D_j \le 7.0$ (depending on the D/D_j ratio). After which, it decreases monotonically. However, the stagnation heat transfer on the smallest cylinder ($D/D_j = 0.5$) behaves in a different manner: fairly constant stagnation heat transfer until $z/D_j = 6.0$, followed by a monotonic decrease.

Studying heat transfer on a flat plate, Gardon and Akfirat [4] observed a similar variation: a monotonic increase up to a point slightly downstream of the potential core. They argued that two conflicting factors – centreline turbulence and the ratio of the arrival velocity at the plate to jet exit velocity, w_o/w_e – are important in dictating the stagnation point heat transfer. Before reaching the tip of the potential core, the centerline velocity is constant whilst the turbulence level along the jet axis keeps increasing. On the other hand, downstream of the potential core, the centreline velocity decays as expressed in Eq. (5), thus reducing heat transfer at the stagnation point. However, the persistently increasing turbulence intensity along the jet axis even after the potential core plays a major role in increasing the stagnation heat transfer, compensating the negative effect of the decayed centreline velocity. This argument of Gardon and Akfirat [4] on the non-monotonic variation of stagnation heat transfer along the jet axis seems to be valid for a circular cylinder subject to a circular impinging jet.

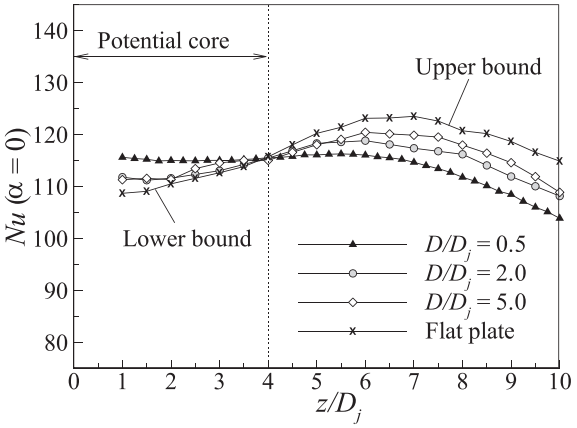

Fig. 6. Nusselt number at the stagnation point ($\alpha = 0°$) plotted as a function of z/D_j for four selected diameter ratios at $Re_j = 20{,}000$.

Fig. 6 also exhibits that inside the potential core, a higher heat transfer at the stagnation point is achievable from the smaller cylinders, whereas the same is obtainable from the larger cylinders outside the potential core. As summarized in Table 1, the existing results on the influence of the diameter ratio on the stagnation heat transfer seem to be conflicting: with the jet Reynolds number fixed, a higher stagnation heat transfer could be observed either on small cylinders [9–11] and or on large cylinders [12–14]. The present heat transfer data clarifies that both the conflicting observations are valid since there is a transition at the tip of the potential core (i.e., $z/D_j = 4.0$). Inside the potential core (i.e., $z/D_j \le 4.0$), the higher heat transfer is obtained from the smaller cylinders, which is consistent with the findings reported in Refs. [9–11]. Heat dissipated from the stagnation point on the flat plate is the lowest (lower bound).

Inside the potential core, a circular cylinder experiences a uniform-like incoming flow, at least, near the stagnation point. Some indication on the effect of a physical cylinder size on the rate of stagnation heat transfer may be inferred from previous studies that dealt with a single cylinder immersed in a uniform free-stream. Overall stagnation heat transfer characteristics are typically correlated as a function of the Reynolds number in the form [19]:

$$Nu_D = C(Re_D)^n \tag{6}$$

where Nu_D is the Nusselt number, C is the empirical constant, Re_D is the Reynolds number, and n is the empirically obtained power index. With the cylinder diameter D selected as a characteristic length, the Nusselt and Reynolds numbers are typically defined respectively as:

$$Nu_D = hD/k_f \tag{7a}$$

and

$$Re_D = \rho U_\infty D/\mu \tag{7b}$$

where U_∞ is the free-stream velocity and h is the convective heat transfer coefficient. Numerous studies suggest that n ranges from 0.33 to 0.8 depending on the Reynolds numbers [19]. From Eqs. (6) and (7a), the convective heat transfer coefficient may be expressed as:

$$h \sim D^{n-1} \tag{8a}$$

so that

$$Nu \sim 1/D^{1-n} \tag{8b}$$

For a given free-stream velocity U_∞ (representing the jet Reynolds number, Re_j), it is evident from Eq. (8b) that the convection heat transfer coefficient (or Nusselt number based on the jet diameter, Nu) at the stagnation point is inversely proportional to the cylinder diameter. This dependence is consistent with both the previous findings [9–11] and the present results for the cylinders positioned inside the potential core.

Farther downstream of the potential core, an opposite dependence of stagnation heat transfer on the diameter ratio is observed. The stagnation heat transfer increases as the diameter of the cylinder is increased, consistent with the observations reported in

Refs. [12–14]. The flat plate results serve the upper bound (Fig. 6). Outside the potential core (e.g., $z/D_j \geq 8.0$), a circular cylinder experiences a non-uniform free-stream flow with its axial velocity varying along the *r*-axis (i.e., the shear flow). The flow acceleration in the vicinity of the stagnation point may play an important role when the cylinder diameter is increased. The shear flow approaching the cylinder has a circulation opposite to that of the boundary layer on the cylinder surface. They interact with each other, affecting the shear stresses on the cylinder surface. Given the heat transfer data in Fig. 6, the local shear stresses near the stagnation point may be increased with increasing cylinder diameter (for a fixed jet diameter), having the maximum value on the flat plate, thus enhancing the stagnation heat transfer. But, this argument needs to be confirmed, which is out of the present scope.

In summary, for a fixed jet Reynolds number, the heat transfer at the stagnation point can be enhanced by either decreasing or increasing the diameter ratio (D/D_j), depending on the impinging distance relative to the potential core. The smaller target cylinders provide a higher stagnation heat transfer if positioned inside the potential core whereas a higher stagnation heat transfer is achievable from the larger cylinders positioned outside the potential core.

3.4. Circumferential heat transfer distribution inside the potential core

The circumferential distribution of convective heat transfer on cylinders positioned inside the potential core is discussed in detail. Fig. 7(a) shows that on a small cylinder ($D/D_j = 0.5$), local transfer coefficient decreases from the stagnation point, reaching a local minimum at $\alpha = 75°$. Afterwards, it is gradually increased. For larger cylinders, a local minimum at $\alpha = 70°$ (for $D/D_j = 2.0$) and $\alpha = 40°$ (for $D/D_j = 5.0$) is formed, followed by a second peak-like local maximum at $\alpha = 100°$ (for $D/D_j = 2.0$) and $\alpha = 45°$ (for $D/D_j = 5.0$), in addition to the primary peak at the stagnation point. After which, the local heat transfer is monotonically decreased.

Overall, the circumferential distribution on these two larger cylinders configurationally is different from that observed from the small cylinder in that a wider circumferential region before the local maximum and a steep decrease in the local heat transfer (as opposed to a gradual increase on the small cylinder). Inside the potential core, the small cylinder ($D/D_j = 0.5$) experiences a uniform-like incoming flow. Therefore, the circumferential heat transfer distribution is expected to follow that of a cylinder immersed in a uniform free-stream, forming a local minimum caused by flow separation [20–22]. To confirm the cause of this local minimum, the static pressure distribution is considered and the results are plotted in Fig. 8. At about $\alpha = 70°$, the point of inflection exists, indicating the occurrence of flow separation.

For a circular impinging jet on a flat plate which is positioned inside the potential core of the jet flow, a local minimum followed by a second peak is typically observed, attributable to the transition from laminar to turbulent flow [2–4]. Fig. 7(b) compares the results with the lateral heat transfer distribution on the flat plate, which exhibits the local minimum formed at $s/D_j = 1.5$. To facilitate the comparison, the abscissa is converted from the azimuth angle to the lateral distance divided by the jet diameter, s/D_j. The heat transfer distribution on the larger cylinders ($D/D_j \geq 2.0$) is similar to that of the flat plate. The lateral location of the local minimum on the two cylinders and the flat plate is consistent i.e., $s/D_j = 1.5$ except for the small cylinder ($D/D_j = 0.5$). Such a consistent lateral location of the local minimum implies that the transition from laminar to turbulent flow is responsible for the local minimum and second peak on the larger cylinders.

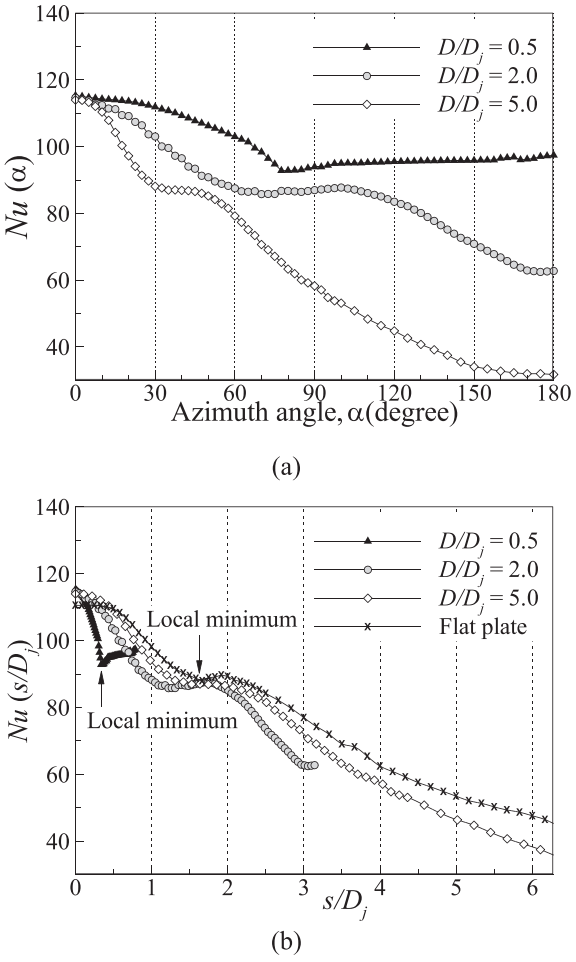

Fig. 7. Measured Nusselt number distribution along the circumference of cylinders at $Re_j = 20{,}000$, positioned inside the potential core region ($z/D_j = 2.0$); (a) Nusselt number vs. Azimuth angle (α); (b) Nusselt number vs. lateral distance (s/D_j).

3.5. Circumferential heat transfer distribution outside the potential core

The cylinders placed downstream of the potential core (i.e., outside the potential core ($z/D_j = 8.0$)) is considered next. The circumferential distributions of heat transfer (Fig. 9) and static pressure (Fig. 10) show that flow separation causes a local

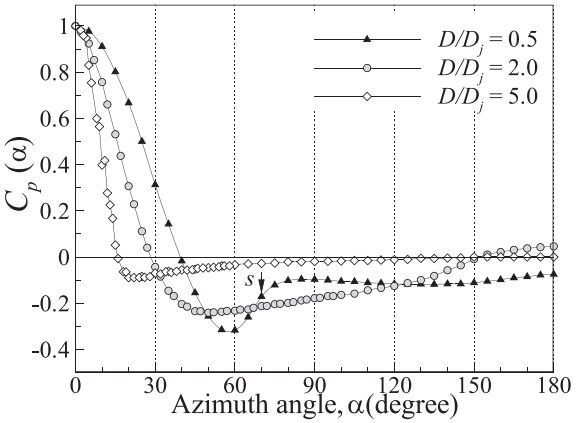

Fig. 8. Measured pressure coefficient distribution along the circumference of cylinders at $Re_j = 20{,}000$ inside the potential core region ($z/D_j = 2.0$).

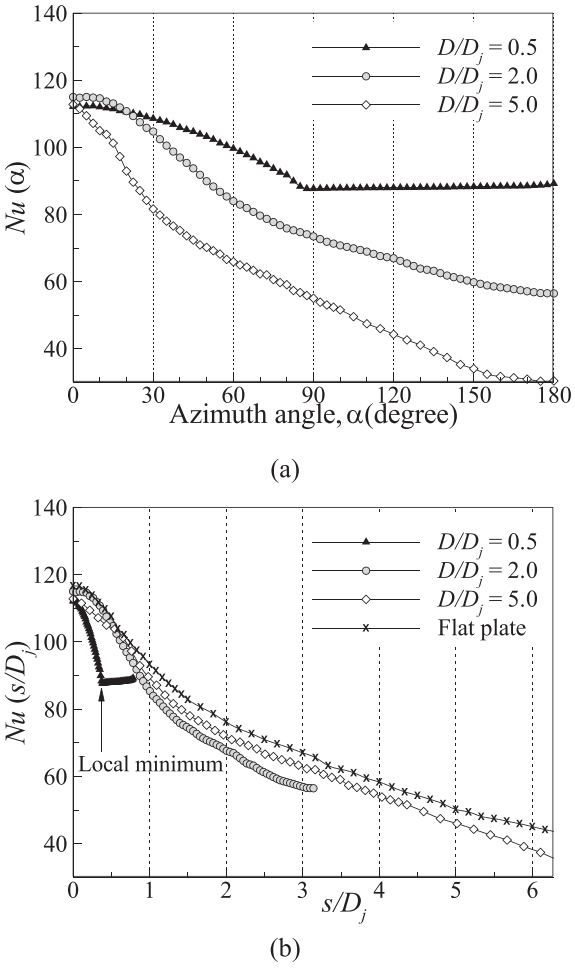

Fig. 9. Measured Nusselt number distribution along the circumference of cylinders at $Re_j = 20{,}000$, positioned outside the potential core ($z/D_j = 8.0$); (a) Nusselt number vs. Azimuth angle (α); (b) Nusselt number vs. lateral distance (s/D_j).

minimum only on the small cylinder ($D/D_j = 0.5$) at about $\alpha = 80°$. Flow separation is slightly delayed from $\alpha = 70°$ to $\alpha = 80°$. At this impinging distance, the incoming flow is typically turbulent in contrast to the laminar incoming flow inside the potential core, which is responsible for the observed delay of flow separation.

For the larger cylinders ($D/D_j \geq 2.0$), the local minimum-like region and second peak (Fig. 9(a)) disappear – a monotonic decrease from the stagnation point. The comparison of the local heat transfer between the cylinders and the flat plate subject to the same circular impinging jet is made in Fig. 9(b). Again, the overall distribution follows that on the flat plate.

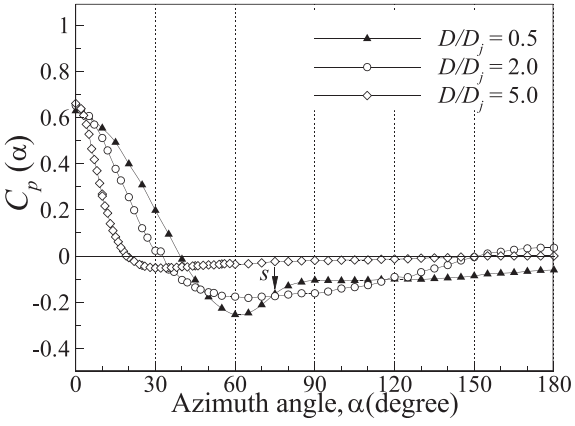

Fig. 10. Measured pressure coefficient distribution along the circumference of cylinders at $Re_j = 20{,}000$ outside the potential core ($z/D_j = 8.0$).

Jambunathan et al. [2] argued the possible causes of the disappeared transition induced second peak based on heat transfer data for a single circular impinging jet on a flat plate as follows. A series of toroidal vortices that form in the shear region around the circumference of the jet are convected downstream. Subsequently, these vortices merge into large vortices and brake down into small-scale random turbulence that penetrates into the jet axis. This penetration causes the radial (or lateral) oscillation of flow on the flat plate, resulting in the break-down of any distinct flow features including the flow transition from laminar to turbulent flows. This argument seems to hold for the present circular jet impinging onto the large cylinders ($D/D_j \geq 2.0$).

4. Conclusions

The details of circumferential heat transfer characteristics on circular cylinders emitting constant heat flux subject to impinging jet cooling in crossflow were experimentally studied for two selected impinging distances distinguished by the potential core of jet flow. With the jet Reynolds number fixed at $Re_j = 20{,}000$, three cylinder-to-jet diameter ratios, $D/D_j = 0.5$, 2.0, and 5.0 were tested. As reference, heat removal from a flat plate (having an infinite radius) by the same circular impinging jet was also measured. The new findings are summarized as follows.

(1) There exists a transition of the dependence of the stagnation point heat transfer rate on the cylinder-to-jet diameter ratio, separated by the potential core.
(2) Inside the potential core, the higher stagnation heat transfer is achievable on the smaller cylinders. On the contrary, outside the potential core the larger cylinders provide the higher stagnation heat transfer.
(3) On the small cylinder ($D/D_j = 0.5$), the local minimum heat transfer is caused as a result of flow separation regardless of the impinging distance.
(4) On the large cylinders ($D/D_j = 2.0$ and 5.0), the formation of the second peak results from the transition from laminar to turbulent flow if positioned inside the potential core. Outside the potential core, the local heat transfer is decreased monotonically from the stagnation point, following that observable on a flat plate.

Acknowledgements

This study was supported by the Korean Ministry of Science and Technology via the South Korea-South Africa Research Center Program (Grant no.: 0420-20110129), by the National Basic Research Program of China (Grant no.: 2011CB610300) and the National 111 Project of China (Grant No.: B06024).

References

[1] H. Martin, Heat and mass transfer between impinging gas jets and solid surfaces, Adv. Heat Transfer 13 (1977) 1–60.
[2] K. Jambunathan, E. Lai, M.A. Moss, B.L. Button, A review of heat transfer data for single circular jet impingement, Int. J. Heat Fluid Flow 13 (1992) 106–115.
[3] J.W. Gauntner, J.N.B. Livingood, P. Hrycak, Survey of Literature on Flow Characteristics of a Single Turbulent Jet Impinging on a Flat Plate, 1970. NASA TN D-5652, NTIS N70-18963.
[4] R. Gardon, J.C. Akfirat, The role of turbulence in determining the heat-transfer characteristics of impinging jets, Int. J. Heat Mass Transfer 8 (1965) 1261–1272.

[5] D. Reungoat, N. Riviere, J.P. Faure, 3C PIV and PLIF measurement in turbulent mixing – round jet impingement, J. Visual.-Japan 10 (2007) 99–110.
[6] H.M. Hofmann, M. Kind, H. Martin, Measurements on steady state heat transfer and flow structure and new correlations for heat and mass transfer in submerged impinging jets, Int. J. Heat Mass Transfer 50 (2007) 3957–3965.
[7] Q.C. Zhang, T.J. Lu, S.Y. He, D.P. He, Control of pore morphology in closed-celled aluminum foams (in Chinese), J. Xian Jiaotong Univ. 41 (2007) 255–270.
[8] Y. Zou, D.P. He, J.Q. Jiang, New type of spherical pore Al alloy foam with low porosity and high strength, Sci. China Ser., B: Chem. 47 (2004) 407–413.
[9] C. Gau, C.M. Chung, Surface curvature effect on slot-air-jet impingement cooling flow and heat-transfer process, J. Heat Transfer-Trans. ASME 113 (1991) 858–864.
[10] C. Cornaro, A.S. Fleischer, M. Rounds, R.J. Goldstein, Jet impingement cooling of a convex semi-cylindrical surface, Int. J. Therm. Sci. 40 (2001) 890–898.
[11] D.H. Lee, Y.S. Chung, D.S. Kim, Turbulent flow and heat transfer measurements on a curved surface with a fully developed round impinging jet, Int. J. Heat Fluid Fl. 18 (1997) 160–169.
[12] E.M. Sparrow, C.A.C. Altemani, A. Chaboki, Jet-impingement heat-transfer for a circular jet impinging in cross-flow on a cylinder, J. Heat Transfer-Trans. ASME 106 (1984) 570–577.
[13] A.A. Tawfek, Heat transfer due to a round jet impinging normal to a circular cylinder, Heat Mass Transfer 35 (1999) 327–333.
[14] D. Singh, B. Premachandran, S. Kohli, Experimental and numerical investigation of jet impingement cooling of a circular cylinder, Int. J. Heat Mass Transfer 60 (2013) 672–688.
[15] H.W. Coleman, W.G. Steele, Experimentation and Uncertainty Analysis for Engineers, John Wiley, New York, 1999.
[16] G.N. Abramovich, The Theory of Turbulent Jets, MIT Press, Cambridge, MA, USA, 1963.
[17] F. Giralt, C.J. Chia, O. Trass, Characterization of impingement region in an axisymmetric turbulent jet, Ind. Eng. Chem. Fund. 16 (1977) 21–28.
[18] E. Esirgemez, J.W. Newby, C. Nott, S.M. Olcmen, V. Otugen, Experimental study of a round jet impinging on a convex cylinder, Meas. Sci. Technol. 18 (2007) 1800–1810.
[19] J.N.B. Livingood, P. Hrycak, Impingement Heat Transfer from Turbulent Air Jets to Flat Plates – A Literature Survey, 1973. NASA Technical Memorandum, NASA TM X-2778.
[20] M.M. Zdravkovich, Flow Around Circular Cylinders, Volume 1: Fundamentals, Oxford University Press, Oxford, 1997.
[21] A. Zukauskas, Heat transfer from tubes in crossflow, Adv. Heat Transfer 18 (1987) 87–159.
[22] E. Schmidt, K. Wenner, Heat transfer over the circumference of a heated cylinder in cross flow, Forsch. Geb. Ing. Wesens 12 (1941) 657–673 (in German).